Agricultural Water Management 186 (2017) 108–119

Contents lists available at ScienceDirect

Agricultural Water Management

journal homepage: www.elsevier.com/locate/agwat

Towards shifting planting date as an adaptation practice for rainfed wheat response to climate change

Milad Nouri[a], Mehdi Homaee[b,*], Mohammad Bannayan[c], Gerrit Hoogenboom[d]

[a] Department of Soil Science, Tarbiat Modares University, P.O. Box 14115-336, Tehran, Iran
[b] Department of Irrigation and Drainage, Tarbiat Modares University, P.O. Box 14115-336, Tehran, Iran
[c] Department of Agronomy, Ferdowsi University of Mashhad, P.O. Box 91775-1163, Mashhad, Iran
[d] Institute for Sustainable Food Systems, University of Florida, FL, USA

ARTICLE INFO

Article history:
Received 27 July 2016
Received in revised form 3 February 2017
Accepted 3 March 2017

Keywords:
CSM-CERES-Wheat
Evapotranspiration
Vapor shift
Water management

ABSTRACT

Maintaining rainfed crop production particularly in water-limited environments is of great importance for agricultural water management under climate change (CC). In such conditions, there is a real demand for finding some practical adaptation scenarios to sustain optimal crop production. This study aimed to investigate the impacts of CC on rainfed wheat yield, transpiration to total evapotranspiration ratio (T/ET) and maximum leaf area index (LAIm) in some semi-arid areas in Iran over 2071–2100 under the current and shifted planting date scenarios. Consequently, the outputs of five climate models under RCP-4.5 and RCP-8.5 emission scenarios downscaled by MarkSimGCM were used to run the CSM-CERES-Wheat v4.6 model. Results revealed that crop yield, T/ET and LAIm will decrease chiefly due to October–November–December (OND) and January–February–March (JFM) precipitation deficit under current sowing date at the most studied sites. Unlike early planting, postponing sowing date from the current to the best date as an adaptive alternative will increase the received precipitation during two early growth phases i.e. germination to terminal spikelet initiation (G-TS) and terminal spikelet to end of leaf growth and beginning of ear growth (TS-ELG). However, a considerable change in the precipitation of entire growing season and grain filling (GF) stage due to delay in sowing date was not projected. Enhanced G-TS rainfall will ensure crop emergence and establishment. Moreover, precipitation increase at TS-ELG phase in which the highest decrease of precipitation was predicted, would enhance LAIm and T/ET. This can be attributed to the fact that the vapor flux in the soil–plant–atmosphere system may shift in favor of transpiration loss through delaying planting date. Therefore, by better matching crop development with changed rainfall distribution, postponing sowing date can partially compensate the deleterious impacts of CC-induced drought on rainfed wheat yield in the west and northwest Iran during 2071–2100.

1. Introduction

Agricultural water management for crop production and food security in water-limited systems is largely influenced by water scarcity and non-water limiting factors such as poor nutrition and salinity (Rockström et al., 2010; Saadat and Homaee, 2015). In arid and semi arid regions, water scarcity (Homaee et al., 2002a,d) and salinity (Homaee et al., 2002b,c; Homaee and Schmidhalter, 2008) are two main important challenges for agricultural water management. Since pre-industrial period, rising atmospheric concentration of greenhouse gases and aerosols mainly due to fossil fuel overuse, land use/cover changes and agricultural activities have triggered anthropogenic global warming and climate change (CC) (IPCC, 2013). Drought exhibited upward trend since 1950 and was projected to be more severe and widespread in the future owing to CC (Dai, 2011, 2013). In the eastern Middle East including the western Iran, meteorological drought would also be more frequent and severe due to declined storm track activity (Evans, 2009). In other words, the already drought prone regions such as Iran are likely to be more liable to CC-related drought (Li et al., 2009).

Being highly vulnerable to meteorological drought, rainfed agriculture is anticipated to be highly impacted by climatic changes particularly in arid and semi-arid regions (Falkenmark, 2013). Producing wheat (*Triticum aestivum L.*), as a primary staple food of billions of people, seems to be highly susceptible to the future CC under rainfed condition in water-limited regions (Anwar et al., 2007; Eyshi Rezaie and Bannayan, 2012; Fischer et al., 2002). Considering increasing trend of environmental and industrial water

* Corresponding author.
E-mail address: mhomaee@modares.ac.ir (M. Homaee).

http://dx.doi.org/10.1016/j.agwat.2017.03.004
0378-3774/

allocation (Faures et al., 2007; Molle et al., 2007), recurrent water stress due to surface and groundwater depletion and projected rainfall deficit, substantial expansion of irrigated lands may not be feasible in the future (Rockström et al., 2010). On the other hand, more agricultural production is needed to guarantee food security of rising population. As a result, management of green water storage (i.e. soil moisture) under rainfed agriculture instead of direct using of blue water (or irrigation) appears to be of high importance not only to achieve food security in a sustainable way, but also not to increase water demand under CC (Rockström et al., 2009; Rockström et al., 2010). In addition, there is a great potential of bridging yield gap (between achieved and potential yield) under rainfed condition through field water management particularly in developing countries (Rockström et al., 2007). Hence, rainfed agriculture will keep playing an important role in meeting food security and coping with CC-induced water shortage (Rockström et al., 2007; Rockström et al., 2010).

Given the importance of rainfed agriculture under future CC and projected rainfed wheat yield loss, adapting wheat cropping system to a drier and warmer climatic condition seems to be a key measure in water-limited areas. It is worth mentioning that adopting adaptation strategies will be more required for the late 21st century in which climatic changes are expected to be stronger (IPCC, 2013). Since the main limiting factor in dryland agriculture is water deficiency, adaptive policies should mainly focus on improving yield through promoting water use efficiency (WUE) rather than using more water (Rockström et al., 2010; Stewart and Steiner, 1990; Yang et al., 2015). At the farm level, manipulating cropping calendar by changing sowing date is one of the adaptive options to alleviate negative impacts of CC on yield (Turral et al., 2011). Better soil water condition at early growing season provided through adjusting planting date improves crop WUE and yield (Turral et al., 2011). Moreover, change in sowing date can shift vapor flux from evaporation (non-productive water loss) to transpiration (productive water loss) in the soil–plant–atmosphere system and enhance green water use efficiency (Rockström, 2003). In other words, CC-induced dry spells can be bridged by shifting planting date (green water management) without using anymore blue water. This would be much more valuable in those courtiers such as Iran which already faced water scarcity and have some potential for enhancing WUE by vapor shift (Rockström et al., 2009).

Hitherto, some studies have been carried out to assess the impacts of shifting sowing date on wheat yield under changing climates (Delécolle et al., 1995; Ghahramani et al., 2015; Rosenzweig, 1990; Southworth et al., 2002; Torriani et al., 2007; Tubiello et al., 2002). The results of these studies indicate that shifting planting date is a region-specific adaptation. The climatic condition may also influence the effectiveness of manipulating sowing date. Weiss et al. (2003) investigated effects of delaying planting date on winter wheat production in two semi-arid and one sub-humid sites located in Nebraska. They concluded that yield loss would decrease in semi-arid and increase in sub-humid areas due to late planting. Delécolle et al. (1995) also pointed out that the effectiveness of changing sowing date highly depends on applied general climate model (GCM) and emission scenario. The effectiveness of adjusting sowing date as an adaptation alternative may, therefore, vary in different regions and also when different GCMs and emission pathways are used. The strategy of shifting planting date should thus be tested for each specific region using an ensemble average of multiple GCMs to reduce projection uncertainty.

This study was aimed (i) to find climate change impacts on rainfed wheat yield, maximum leaf area index (LAIm) and transpiration to evapotranspiration ratio (T/ET) during the 2080s (2071–2100) in the west and northwest of Iran and (ii) to evaluate the influence of shifting sowing date as an adaptation measure on wheat grain yield, T/ET, LAIm and precipitation quantity at five different wheat phenological stages.

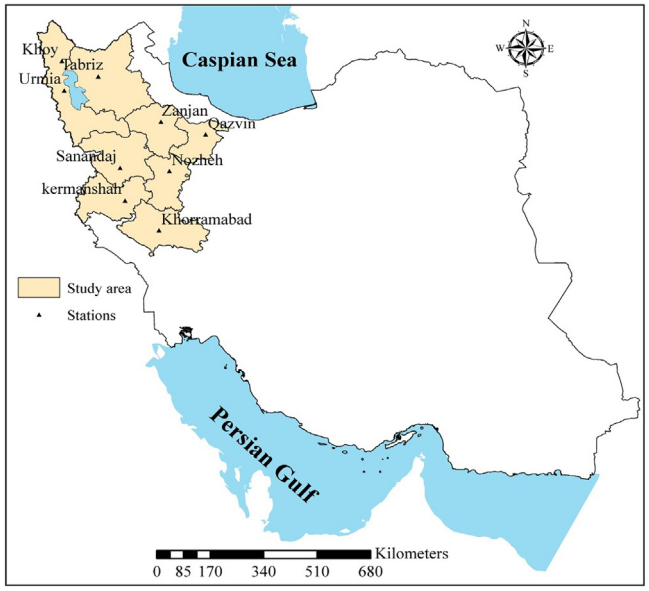

Fig. 1. The study areas located in the west and northwest of Iran.

2. Materials and methods

2.1. Study area

Iran has a wide range of climatic conditions mainly due to existence of the Alborz and the Zagros mountain ranges. Rain producing air masses predominantly enter from the west and northwest of the country causing above-average rainfall (300–500 mm annual precipitation) in the western half of the country owing to the Zagros mountain chain geographical location. Consequently, a semi-arid climate mostly dominates in the west and northwest of Iran. The local map of the study area is depicted in Fig. 1. The climate of all studied sites is categorized as semi-arid according to UNEP (1997). Semi-arid climatic condition as well as fertile plains have made the western half of Iran an appropriate area for rainfed agriculture. Around 75% of all rainfed wheat produced in Iran is harvested from the fields located in the studied regions (Ministry of Agriculture, 2011). Annual average rainfed wheat yield in the studied area is approximately 900 kg ha^{-1}.

2.2. Data

2.2.1. Climatic data

In this study, MarkSimGCM was employed to downscale coarse-scale GCMs (General Circulation Models) outputs to a $0.5^{\circ} \times 0.5^{\circ}$ latitude/longitude grid resolution using stochastic downscaling and climate typing techniques (Jones and Thornton, 2013). MarkSimGCM generates rainfall data based on third-Markov stochastic model and daily temperature (minimum and maximum) as well as solar radiation data using Richardson (1981) approach. Further, MarkSimGCM collects the baseline period climate data (1961–1990) from the WorldClim database. The model has been employed to downscale GCMs outputs in different climates over the globe (Fouial et al., 2016; Liu et al., 2016; Mathukumalli et al., 2016; Nouri et al., 2016; Shirsath et al., 2017). Nouri et al. (2016) showed that MarkSimGCM can successfully produce the required climate data for agrohydrological modeling over Iran. For our assessment, an ensemble mean of five GCMs participating in the fifth phase of Coupled Model Intercompar-

Table 1
The physical properties of soils, averaged over all layers, used in the study.

Soil series	Site	Sand (%)	Silt (%)	Clay (%)	θ_s [b,a] (%)	LL[c,a] (%)	DUL[d,a] (%)	OC[e] (%)	ρ_b [f] (g cm^{-3})	K_s [a,g] (cm h^{-1})
Osko	Tabriz	61.0	24.0	15.0	40	10.7	20.1	0.22	1.49	2.59
Qaratapeh	Khoy	20.4	54.5	25.1	48	16.0	31.5	0.36	1.35	0.53
Emam Kandi	Urmia	52.4	21.4	26.2	38	14.7	25.1	0.80	1.45	0.82
Ideloo	Nozheh	25.4	41.1	33.5	47	20.0	33.9	0.23	1.29	0.23
Qeidar	Zanjan	21.2	40.3	38.5	45	16.4	33.4	0.40	1.36	0.59
Kuien	Qazvin	33.2	36.9	29.8	44	18.1	31.0	0.30	1.39	0.50
Serjineh pain	Sanandaj	27.2	34.2	38.6	44	22.4	35.5	0.60	1.37	0.10
Seifabad	Khorramabad	14.2	52.0	33.8	47	20.9	37.7	0.50	1.40	0.17
Amleh	Kermanshah	30.4	28.0	41.6	47	26.5	40.6	1.30	1.32	0.12

[a] Determined based on pedo-transfer functions.
[b] Saturation.
[c] Lower limit of water availability.
[d] Drained upper limit.
[e] Organic carbon content.
[f] Soil bulk density.
[g] Saturated hydraulic conductivity.

Table 2
Genetic parameters of Azar-2 wheat cultivar for the CSM-CERES-Wheat model.

Genetic coefficients	Description	Value
P1V	Days at optimum vernalizing temperature required for completing vernalization	7
P1D	Photoperiod (pp) response (% reduction in rate/10 h drop in pp)	30
P5	Grain filling (excluding lag) phase duration (°C d)	510
G1	Kernel number per unit canopy weight at anthesis (#/g)	11
G2	Standard kernel size under optimum conditions (mg)	36
G3	Standard, non-stressed mature tiller weight (including grain) (g dry weight)	2
PHINT	Interval between successive leaf tip appearances (°C d)	57

ison Project (CMIP5) (IPCC, 2013), i.e. BCC-CSM 1.1(m) (Beijing Climate Center, Climate System Model, version 1.1 (moderate resolution), 2.81° × 2.81° latitude/longitude) (Wu, 2012), FIO-ESM (First Institute of Oceanography-Earth System Model, 2.81° × 2.81° latitude/longitude) (Song et al., 2012), GFDL-ESM2M (Geophysical Fluid Dynamics Laboratory Earth System Model with MOM, version 4 component, 2° × 2.5° latitude/longitude) (Dunne et al., 2012), (Institut Pierre-Simon Laplace Coupled Model, version 5A, low resolution, 1.87° × 3.75° latitude/longitude) (Dufresne et al., 2013) and MIROC-ESM-CHEM (Model for Interdisciplinary Research on Climate, Earth System Model, Chemistry Coupled, 2.81° × 2.81° latitude/longitude) (Watanabe et al., 2011) under RCP-4.5 and RCP-8.5 (Representative Concentration Pathways) were used for future climate condition. RCP-4.5 and RCP-8.5 scenarios represent mitigated and unmitigated emission pathways in the future, respectively. In this study, daily climatic data were synthesized for 30 replicates (different weather years) in the baseline and future time slices. More details on the selected GCMs and RCPs are given by Flato et al. (2013), Collins et al. (2013), Riahi et al. (2011) and Thomson et al. (2011).

2.2.2. Soil data

The soil data required for the CSM-CERES-Wheat (Cropping System Model-Crop Environment Resource Synthesis-Wheat) (Jones et al., 2003) model are the lower limit of water availability to plants (LL, %), drained upper limit (DUL, %), saturation (θ_s, %), saturated hydraulic conductivity (K_s, cm h^{-1}) and soil root growth factor (SRGF) (Ritchie, 1998). Since measuring these parameters are often tedious and time-consuming, a set of pedo-transfer functions developed by Rawls et al. (1982) and Saxton et al. (1986) are included in DSSAT v4.6 (Decision Support System for Agrotechnology Transfer) (Hoogenboom et al., 2014) to predict the required soil physical properties. The readily available soil characteristics (i.e. particle size distribution, bulk density (ρ_b) and organic carbon (OC)) for the dominant soil series in each location were obtained from soil and land use reports and maps provided by Iran Soil and Water Research Institute (Table 1).

2.2.3. Crop data

A winter bread wheat cultivar (Azar-2) commonly grown under rainfed condition in the west of Iran was considered in this study. The required data for calibrating and evaluating the CSM-CERES-Wheat were obtained from a two-years experiment conducted in three sites located in Azarbayejan-e-Sharghi (Maragheh) (37° 9′ °N, 46° 9′ °E, 1720 m.a.s.l), Kordestan (35° 12′ °N, 47° 00′ °E, 1500 m.a.s.l) and Zanjan (36° 24′ °N, 48° 17′ °E, 1662 m.a.s.l) (Feiziasl et al., 2007). The experiments were carried out employing four nitrogen rates (0, 30, 60 and 90 kg N ha^{-1}), two nitrogen fertilizer types (Urea and Ammonium nitrate) each with three replicates during two years (2002–2003 and 2003–2004). In Maragheh station, two types of N-fertilizer application including all-autumn and autumn-spring split were performed. Grain yield, thousand kernel weight (TKW), days to maturity (DMA) and days to flowering (DFW) were the data used for calibration and evaluation of the model. The first-year data set including 28 sets of data was used for calibration. The second-year data including 28 sets of data was also considered for model evaluation. The Genotype Coefficient Calculator (Genecalc) software included in DSSAT v4.6 was used to estimate the genetic coefficients of Azar-2 cultivar as depicted in Table 2. The planting method (dry seed), planting depth (5 cm), planting distribution (rows), fertilizer applications (60 kg urea-N ha^{-1}), row spacing (25 cm) and plant population at seeding (350 per m^2) were obtained based on several experiments performed in Iranian Dryland Agricultural Research Institute (DARI). Furthermore, planting dates were considered to be 1 November in Khorramabad, 15 October in Qazvin and Kermanshah and 7 October in other stations recommended by DARI (DARI, 2014).

2.3. Modeling

The CSM-CERES-Wheat model included in DSSAT v4.6 was used in this study to project grain yield, evapotranspiration compo-

nents and LAI under CC. The CSM-CERES-Wheat is a field-scale, daily-scale, one dimensional and ecophysiological model which simulates wheat growth as well as soil moisture and nitrogen budget and dynamics. The model partitions potential evapotranspiration (ET_0) into potential soil evaporation (E_0) and potential crop transpiration (T_0) based on the fraction of solar energy reaching the soil surface and LAI (Jones et al., 2003). The CSM-CERES-Wheat calculates soil evaporation in a two-stage process (Ritchie, 1972). The potential plant transpiration (T_0) is also computed based on an extinction coefficient (k) and the given LAI values (Ritchie, 1972; Sau et al., 2004).

The CSM-CERES-Wheat model classifies the wheat growing season into nine stages including fallow or presowing (stage 7), sowing to germination (S-G, stage 8), germination to emergence (G-E, stage 9), emergence to terminal spikelet initiation (E-TS, stage 1), terminal spikelet to end of leaf growth and beginning of ear growth (TS-ELG, stage 2), end of leaf growth and beginning of ear growth to end of pre-anthesis ear growth (ELG-EEG, stage 3), end of pre-anthesis ear growth to beginning of grain filling (EEG-BGF, stage 4) and grain filling (GF, stage 5) (Ritchie, 1991). Wheat growth and development primarily occurs within germination to terminal spikelet initiation (G-TS), TS-ELG, ELG-EEG, EEG-BGF and GF phases (Ritchie, 1991). In this study, the average CO_2 concentrations for simulations under RCP-4.5 and RCP-8.5 in 2071–2100 were considered to be 532 and 802 ppmv, respectively (IPCC, 2013).

2.4. Adaptation option

In order to assess the influence of shifting planting date and identify the best planting date (BPD) in the 2080s, the sowing date was changed in a weekly interval from 1 October to 1 December. It should be noted that more severe climate change projected for the 2080s would make the adaptive strategies more necessary in the late 21 century. BPD is the onset date of the growing season in

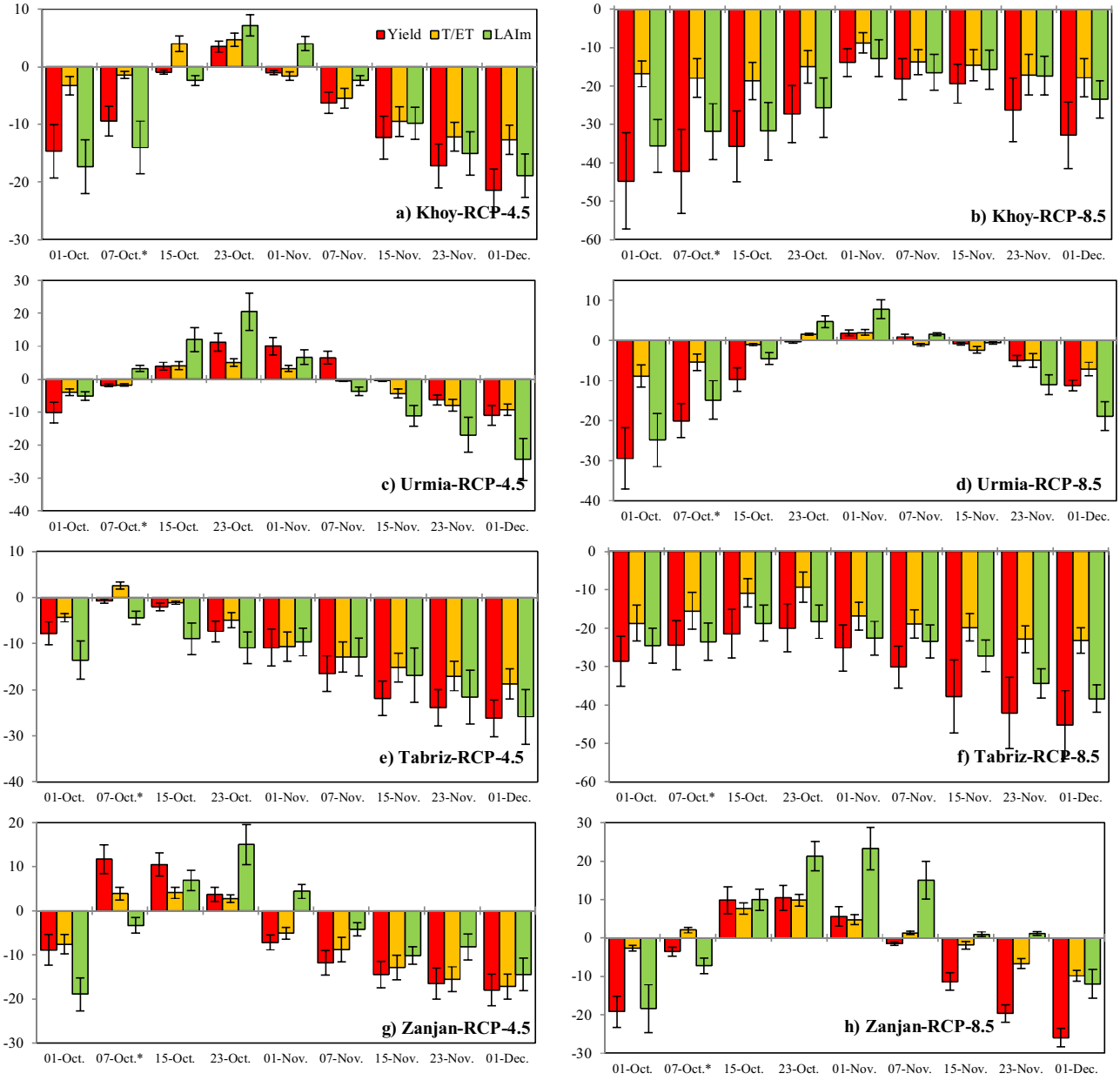

Fig. 2. The changes (%) in wheat yield (Y), transpiration to evapotranspiration (T/ET) and maximum leaf area index (LAIm) over a wide range of planting dates under RCP-4.5 and 8.5 in the 2080s relative to the baseline. (The asterisk denotes the current sowing date. Error bars represent the standard deviation of the projections).

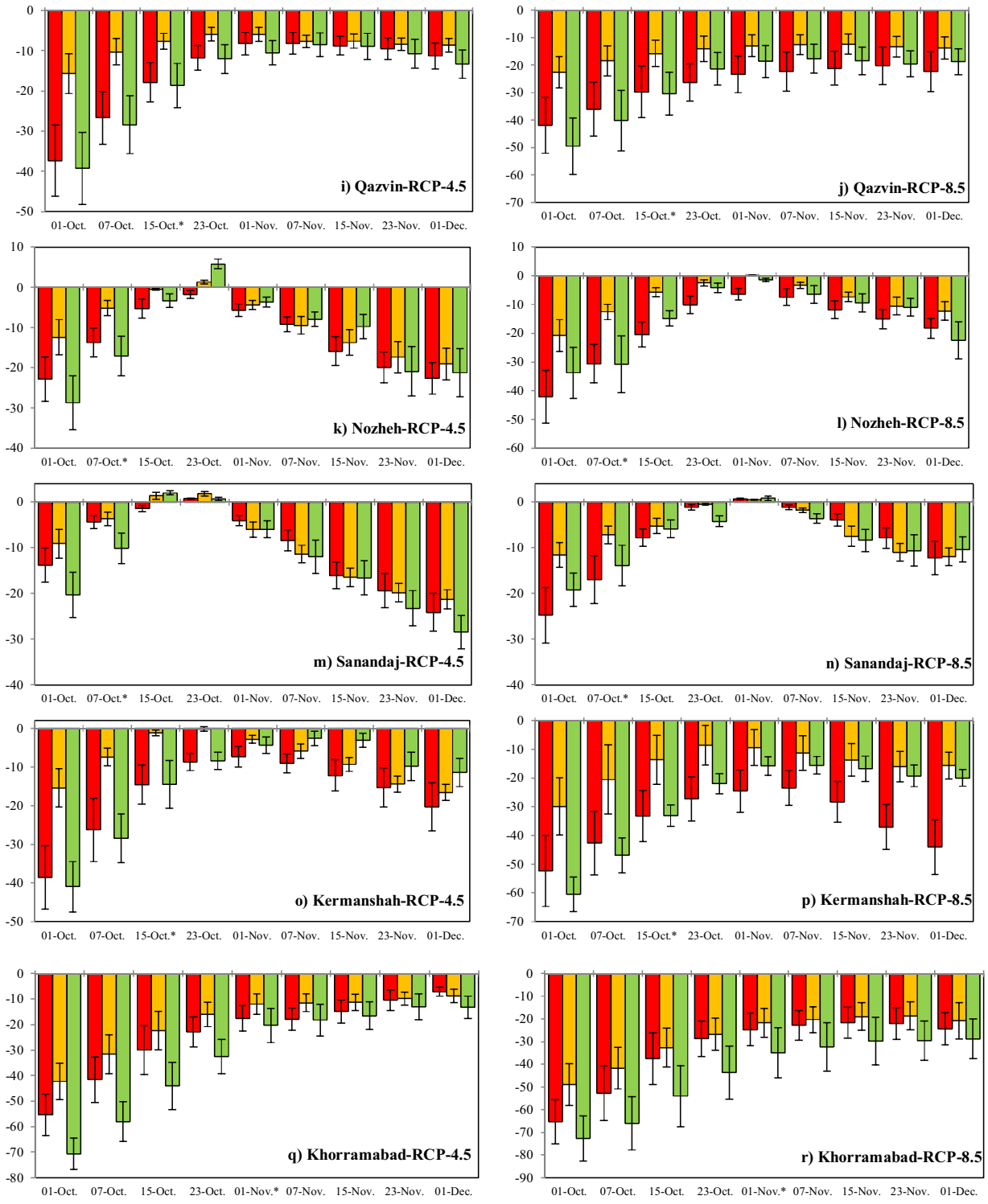

Fig. 2. (*Continued*)

which the highest grain yield would be attained. Advancing sowing date of wheat under rainfed condition to September seems not to be a viable and realistic adaptation. Because the rainfall in September is insufficient to guarantee crop establishment in the study area. Planting rainfed wheat later than 1 December may also cause a severe terminal drought. Furthermore, sowing too early (in September) or too late (in December) would also restrict cropping summer crops in rotation with rainfed wheat. As a result, the considered sowing date window seems to be logistically reasonable and applicable.

2.5. Quantitative evaluation of model performance

The performance of the CSM-CERES-Wheat model for calibration and evaluation periods was assessed using three statistics including normalized root mean square error (nRMSE), means bias

Table 3
The obtained statistics for evaluating CSM-CERES-Wheat performance.

Variable	Set of data	ObservationMean[g]	nRMSE[a] (%)	MBE[b,g]	d_r [c] (–)
Grain yield	Calibration	1985.3	14.3	−76.7	0.64
	Validation	2476.3	16.4	−107.8	0.55
TKW[d]	Calibration	39.5	7.0	−0.9	0.41
	Validation	47.5	10.1	−3.5	0.16
DMA[e]	Calibration	231.5	4.0	3.0	0.49
	Validation	244.8	7.6	1.9	0.48
DFW[f]	Calibration	187.4	3.5	2.4	0.68
	Validation	203.7	7.9	3.2	0.47

[a] Normalized root mean square.
[b] Mean bias error.
[c] Refined Willmott's index.
[d] Total kernel weight.
[e] Days to maturity.
[f] Days to flowering.
[g] MBE and observation mean units for Grain yield, TKW, DMA and DFW are kg, g, day and day, respectively.

error (MBE) and refined Willmott's index (d_r). The mathematical expressions of these statistics are (Nouri et al., 2014):

$$\mathrm{MBE} = 1/n\sum_{i=1}^{n}(S_i - O_i) \quad (1)$$

$$\mathrm{nRMSE} = \frac{100}{\overline{O}}\sqrt{\left(\sum_{i=1}^{n}(S_i - O_i)^2\right)/n} \quad (2)$$

$$d_r = \begin{cases} 1 - \left\{\sum_{i=1}^{n}|P_i - O_i| / c\sum_{i=1}^{n}|O_i - \overline{O}|\right\}, & if \ \sum_{i=1}^{n}|P_i - O_i| \le c\sum_{i=1}^{n}|O_i - \overline{O}| \\ \left\{c\sum_{i=1}^{n}|O_i - \overline{O}| / \sum_{i=1}^{n}|P_i - O_i|\right\} - 1, & if \ \sum_{i=1}^{n}|P_i - O_i| > c\sum_{i=1}^{n}|O_i - \overline{O}| \end{cases} \quad (3)$$

where S_i is the simulated values, O_i is the observed values, $\bar{O}$ is mean of the observations, c equals to 2 and n is the number of time steps.

The normalized root mean square error (nRMSE) is frequently used to characterize the differences between the simulated and recorded values in the agrohydrology literature (Homaee et al., 2002a; Zarei et al., 2010). The model performance is considered perfect with nRMSE value less than 10%, good if nRMSE is between 10% and 20%, fair if nRMSE is between 20% and 30% and poor if nRMSE quantity is greater than 30% (Dettori et al., 2011). MBE is an index quantifying model bias and systematic error and its negative (positive) values indicate model tendency to underestimate (overestimate) (Willmott, 1982). d_r is a dimensionless relative error or goodness-of-fit measure varying between −1 and 1 (Willmott et al., 2012). If the simulated values are equivalent to the observations ($S_i = O_i$), the model performance is excellent and the magnitude of d_r statistic is one and the quantity of MBE and nRMSE statistics are equal to zero.

3. Results and discussions

3.1. The CSM-CERES-Wheat evaluation

Considering the obtained nRMSE values (10% < nRMSE < 20%), the CSM-CERES-Wheat provided a good estimate of grain yield in both calibration and testing periods (Table 3). The simulation accuracy of the model was also excellent (nRMSE < 10%) for days to maturity (DMA) and days to flowering (DFW) during both phases and for thousand kernel weight (TKW) over the calibration period. Given MBE values, the model often tended to underestimate grain yield (3.8 and 4.3% of the mean of observed value) and TKW (2.2 and 7.3% of the mean of observed value), while overestimate DMA (1.3 and 0.8% of the mean of observed value) and DFW (1.3 and 1.6% of the mean of observed value). Furthermore, the close to 0.5 values for d_r illustrated that sum of the error-magnitudes was approximately one half of the sum of perfect modeled and recorded grain yield, DMA and DFW deviations (Willmott et al., 2012). In the testing phase, as the value of absolute error indicated good estimation of TKW (10% < nRMSE < 20%), low value of d_r for TKW can be attributed to low variation of recorded data (Willmott et al., 2012).

3.2. Future changes in climate

Averaged across all sites, an increase of 2.3 and 4.8 °C in annual T_{min} and 2.9 and 5.6 °C in annual T_{max} was projected under RCP-4.5 and RCP-8.5, respectively (Tables 4 and 5). On monthly scale, increase of average T_{min} (°C) would likely range from 1.7 (in March) to 3.3 (in September) for RCP-4.5 and from 3.8 (in January) to 6.3 (in March) for RCP-8.5. Furthermore, the average T_{max} increment (°C) will likely be in range of 2.2 (in March) to 3.8 (in September) under RCP-4.5 and 4.6 (in January) to 6.5 (in September) under RCP-8.5. The average annual precipitation reduction is expected to be 8.3 and 12.3% under RCP-4.5 and 8.5, respectively, in the 2080s with respect to the baseline. Mean dry spell length will be increased by 10.0 and 11.7%, averaged across all stations, for RCP-4.5 and 8.5, respectively. The average increase of OND, JFM and AMJ mean dry spell length was, respectively, 5.3, 9.2 and 12.0% under RCP-4.5 and 5.0, 17.1 and 35.4% under RCP-8.5. Consequently, it is anticipated that the west and northwest regions of Iran would receive lower precipitation and most likely experience more and longer droughts (Tables 4 and 5).

3.3. The CC-induced changes in grain yield, T/ET and LAIm under current planting date

Wheat yield under the current planting date (CPD) is likely to be reduced in all stations for both RCPs except in Zanjan under RCP-4.5 (Fig. 2). The highest reduction of wheat yield was projected in Qazvin (17.8%) under RCP-4.5 and Khoy (42.3%) under RCP-8.5 in the 2080s relative to the baseline. A decline in transpiration to total evapotranspiration (T/ET) was projected in all scenarios and stations expect for Tabriz under RCP-4.5 and Zanjan for both RCPs under CPD (Fig. 2). An average decrease of 2.9 and 11.9% in T/ET was modeled under RCP-4.5 and 8.5, respectively. Moreover, LAIm will decrease in all cases under CPD except for Urmia under RCP-

Table 4
Average change of monthly, annual and seasonal (OND, JFM and AMJ) T_{min} (°C), T_{max} (°C), precipitation (%) and mean dry spell length (DSL) (%) in the 2080s (ensemble average) relative to the baseline period under RCP-4.5.

Station	Variable	Jan.	Feb.	Mar.	Apr.	May.	Jun.	Jul.	Aug.	Sep.	Oct.	Nov.	Dec.	OND[a]	JFM[b]	AMJ[c]	Annual
Khoy	ΔT_{min}	2.2	2.1	2.0	2.1	2.0	2.6	3.1	3.4	3.4	2.6	2.0	2.0	2.2	2.1	2.2	2.5
	ΔT_{max}	2.6	2.8	2.4	2.9	2.9	3.5	3.8	3.9	4.0	3.0	2.4	2.3	2.5	2.6	3.1	3.0
	ΔP	−5.9	−34.5	−14.8	−20.5	4.4	−18.8	−30.6	−15.2	8.1	2.0	−16.6	−33.9	−13.9	−19.2	−7.6	−12.4
	ΔDSL	15.9	−3.4	11.7	13.1	−1.8	30.8	32.8	−0.7	2.9	−3.1	2.5	11.0	4.1	7.9	17.1	11.7
Urmia	ΔT_{min}	2.4	2.0	1.9	2.0	2.2	2.8	3.2	3.3	3.5	2.7	1.9	2.1	2.2	2.0	2.3	2.5
	ΔT_{max}	2.6	2.7	2.2	2.8	3.1	3.7	3.7	3.8	4.1	3.1	2.5	2.5	2.7	2.5	3.2	3.1
	ΔP	−12.0	−5.5	0.4	10.3	−12.7	−16.5	−51.0	−22.0	49.3	4.4	−4.1	−13.5	−4.5	−4.9	−3.4	−4.1
	ΔDSL	−4.0	−3.1	4.0	33.7	−3.1	0.0	17.8	−2.3	−1.8	10.9	4.5	10.7	9.0	−1.2	6.6	7.5
Tabriz	ΔT_{min}	2.0	1.9	1.8	2.0	2.2	2.7	3.0	3.2	3.3	2.6	1.8	2.0	2.1	1.9	2.3	2.4
	ΔT_{max}	2.4	2.7	2.2	2.7	2.9	3.5	3.5	3.8	3.8	3.0	2.4	2.3	2.6	2.4	3.0	2.9
	ΔP	−15.5	−9.1	5.2	−2.5	−3.2	−57.4	−51.6	−16.5	−20.7	17.8	−27.5	−9.2	−4.6	−4.5	−13.2	−9.4
	ΔDSL	19.5	24.9	7.9	17.3	−15.3	7.8	24.6	4.2	−12.0	−15.1	13.0	5.6	1.4	17.8	4.4	6.7
Zanjan	ΔT_{min}	1.6	1.5	1.6	2.0	2.2	2.4	2.6	2.9	3.2	2.4	2.0	1.7	2.0	1.6	2.2	2.2
	ΔT_{max}	2.1	2.2	2.0	2.8	2.8	3.0	3.1	3.2	3.6	2.8	2.3	2.4	2.5	2.1	2.9	2.7
	ΔP	1.3	16.7	0.6	−30.2	−1.7	−36.0	−36.6	−27.3	−58.6	−5.3	−7.2	−2.9	−4.6	5.7	−16.8	−6.7
	ΔDSL	3.9	7.5	−3.0	−7.0	16.5	29.8	24.7	2.1	29.0	−13.3	3.7	16.7	−0.2	2.8	18.8	11.3
Nozheh	ΔT_{min}	1.7	1.7	1.6	2.0	2.4	2.7	2.7	3.0	3.3	2.6	2.0	2.0	2.2	1.6	2.4	2.3
	ΔT_{max}	2.4	2.5	2.2	3.0	3.3	3.2	3.3	3.2	3.8	3.1	2.4	2.6	2.7	2.4	3.2	2.9
	ΔP	−17.6	−14.5	−14.5	9.0	−20.3	7.7	−45.9	339.4	113.0	−7.0	10.7	−7.8	−0.3	−15.5	−5.6	−7.4
	ΔDSL	19.5	13.0	15.1	13.3	20.8	1.0	11.9	−24.6	−17.6	4.1	8.1	18.0	9.4	16.0	6.8	12.9
Qazvin	ΔT_{min}	1.5	1.6	1.7	2.1	2.3	2.4	2.5	2.7	2.9	2.2	1.8	1.6	1.8	1.6	2.3	2.1
	ΔT_{max}	2.1	2.4	2.1	2.9	3.0	3.0	3.1	3.1	3.3	2.5	2.1	2.1	2.2	2.2	2.9	2.6
	ΔP	−27.8	−11.2	−11.4	−15.7	−29.9	−41.7	−0.8	−87.8	4.7	34.7	−5.1	−21.6	−4.6	−14.8	−21.9	−14.4
	ΔDSL	18.1	−4.6	−25.3	−7.5	12.1	17.1	−4.3	8.7	7.3	−7.7	0.8	−3.3	−3.6	−2.9	11.5	−1.6
Sanandaj	ΔT_{min}	1.8	1.7	1.8	2.3	2.6	2.9	2.9	2.9	3.3	2.6	1.9	1.9	2.1	1.7	2.6	2.4
	ΔT_{max}	2.5	2.6	2.4	3.2	3.4	3.6	3.5	3.2	3.7	2.8	2.2	2.4	2.5	2.5	3.4	3.0
	ΔP	−4.1	0.6	−10.1	−7.4	−22.4	−42.1	20.0	−70.3	−11.1	24.7	15.9	−11.7	6.3	−4.7	−15.9	−5.8
	ΔDSL	5.0	11.6	13.5	8.0	18.8	22.0	−3.1	−7.6	−0.3	−1.3	5.9	13.4	5.1	10.1	18.8	10.3
Kermanshah	ΔT_{min}	1.8	1.5	1.6	2.2	2.5	2.7	2.8	3.0	3.5	2.8	2.0	1.9	2.2	1.6	2.4	2.4
	ΔT_{max}	2.6	2.4	2.2	3.0	3.2	3.3	3.3	3.2	3.8	3.1	2.6	2.7	2.8	2.4	3.2	2.9
	ΔP	0.2	−30.5	−9.5	−22.9	−18.0	−22.5	246.9	11.1	56.5	41.4	−6.9	−9.8	−2.6	−12.8	−20.6	−11.1
	ΔDSL	0.1	5.9	6.2	2.1	17.3	5.1	−3.7	−1.9	−0.9	1.0	8.7	5.9	4.2	4.2	6.9	5.4
Khorramabad	ΔT_{min}	1.8	1.7	1.6	2.3	2.6	2.6	2.7	2.9	3.4	2.9	2.2	2.0	2.4	1.7	2.5	2.4
	ΔT_{max}	2.7	2.4	2.1	3.0	2.9	3.1	3.2	3.1	3.8	3.1	2.7	2.6	2.8	2.4	3.0	2.9
	ΔP	−4.8	−1.1	−6.2	16.0	−6.5	29.5	422.0	−35.7	−39.4	26.1	−16.0	−15.0	−10.3	−4.2	7.1	−3.7
	ΔDSL	46.8	27.6	14.2	25.3	24.5	11.7	−16.5	6.0	6.7	1.0	28.0	40.5	18.1	28.4	16.9	26.0

[a] October–November–December.
[b] January–February–March.
[c] April–May–June.

4.5 (Fig. 2). Averaged across all locations, a decline of 11 and 24.5% in LAIm was projected under RCP-4.5 and RCP-8.5, respectively. The largest decrease in T/ET and LAIm was predicted for Khorramabad site (Fig. 2). The rainfall deficit during the growing season (Tables 4 and 5) is expected to result in decreased LAIm (aboveground and leaf biomass), T (T/ET) and grain yield. In some sites such as Sanandaj, Tabriz and Urmia for RCP-4.5 and Zanjan under RCP-8.5, crop yield would be declined by 4% ≥ in the 2080s relative to the baseline (Fig. 2). An increase or a slight decrease of rainfall (5% >) in the OND and JFM seasons in addition to CO_2 fertilization can account for negligible crop yield loss in these cases, despite an over 13% reduction in the AMJ rainfall in some cases. This implies that precipitation received during the OND and JFM seasons are of great importance to maintain rainfed wheat yield under CC in the studied area.

3.4. Impacts of shift in sowing date upon yield, T/ET and LAIm

Planting wheat earlier than CPD is expected to decrease yield in all sites located in the studied area (Fig. 2). Unlike advancing sowing date, rainfed wheat yield can be increased through late planting (Fig. 2). A 2-week delay of seeding may promote grain yield (kg ha^{-1}) by 177.0 in Khoy, 219.6 in Urmia, 167.1 in Qazvin, 220.8 in Nozheh, 93.3 in Sanandaj and 173.5 in Kermanshah for RCP-4.5 (Fig. 2a, c, i, k, m and o). Furthermore, sowing 4 weeks later than CPD is expected to enhance wheat yield by 181.9 (kg ha^{-1}) under RCP-4.5 in Khorramabad during the 2080s (Fig. 2q). Increasing yield through delaying planting date in Tabriz and Zanjan under RCP-4.5 seems to be unlikely (Fig. 2e and g). Under RCP-8.5, delaying sowing date by 3 weeks can increase wheat yield (kg ha^{-1}) by 388.8 in Khoy, 370.5 in Urmia, 448.1 in Nozheh, 323.5 in Sanandaj and 234.0 in Kermanshah (Fig. 2b, d, l, n and p). In addition, a 2-week delay in planting appears to increase yield (kg ha^{-1}) by 61.3 in Tabriz and 230.5 in Zanjan under RCP-8.5 in the last decades of 21st century (Fig. 2f and h). A 5-week delay of sowing date will improve crop yield by 166.1 kg ha^{-1} in Qazvin for RCP-8.5 (Fig. 2j). Overall, shifting from CPD to BPD would enhance yield by 176.2 and 252.9 kg ha^{-1}, averaged across all sites, for RCP-4.5 and RCP-8.5, respectively, in 2071–2100.

Averaged across all sites, shifting from CPD to BPD will increase T/ET ratio (mm mm^{-1}) by 0.024 and 0.038 and LAIm (m^2 m^{-2}) by 0.58 and 0.70 for RCP-4.5 and 8.5, respectively (Fig. 2). The greatest increment of T/ET (mm mm^{-1}) caused by shifting from CPD to BPD was 0.040 and 0.079 for RCP-4.5 and RCP-8.5, respectively, at Nozheh followed by 0.039 under RCP-4.5 in Urmia and 0.050 under RCP-8.5 in Zanjan. The greatest LAIm enhancement (m^2 m^{-2}) due to shifting from CPD to BPD was 0.84 and 1.10 for RCP-4.5 and RCP-8.5,

Table 5
Average change of monthly, annual and seasonal (OND, JFM and AMJ) T_{min} (°C), T_{max} (°C), precipitation (%) and mean dry spell length (DSL) (%) in the 2080s (ensemble average) relative to the baseline period under RCP-8.5.

Station	Variable	Jan.	Feb.	Mar.	Apr.	May.	Jun.	Jul.	Aug.	Sep.	Oct.	Nov.	Dec.	OND[a]	JFM[b]	AMJ[c]	Annual
Khoy	ΔT_{min}	4.3	4.4	4.0	4.0	4.1	5.1	6.2	6.5	6.4	5.4	4.2	4.2	4.6	4.2	4.4	4.9
	ΔT_{max}	4.9	5.6	5.1	5.4	5.4	6.8	7.1	7.0	6.8	5.8	5.3	5.1	5.3	5.2	5.8	5.8
	ΔP	−40.7	−25.8	−34.8	−46.6	−3.0	−69.4	−52.6	39.8	76.4	0.2	−26.1	−59.6	−24.5	−33.4	−27.8	−24.1
	ΔDSL	52.6	1.9	−1.0	11.6	−21.2	95.4	55.3	−12.1	−24.3	−22.4	−6.7	60.7	15.3	16.2	39.9	9.8
Urmia	ΔT_{min}	4.5	4.2	3.9	4.0	4.5	5.4	6.3	6.5	6.7	5.6	4.3	4.3	4.7	4.2	4.7	5.0
	ΔT_{max}	5.0	5.4	5.0	5.3	5.8	6.8	7.1	6.9	6.9	6.0	5.3	5.4	5.5	5.1	6.0	5.9
	ΔP	−31.1	−7.8	−13.5	−34.0	−19.7	−63.8	−62.1	39.1	89.8	−9.6	−8.3	−47.1	−20.4	−16.4	−32.3	−20.4
	ΔDSL	14.7	2.1	19.0	19.0	−21.0	36.4	37.9	1.6	−34.2	−11.6	−18.2	25.4	1.4	12.2	17.5	11.4
Tabriz	ΔT_{min}	3.9	4.1	3.9	4.0	4.4	5.4	6.1	6.2	6.1	5.1	4.0	4.0	4.3	3.9	4.6	4.8
	ΔT_{max}	4.5	5.3	5.1	5.5	5.4	6.9	6.9	6.7	6.5	5.4	4.8	5.0	5.0	5.0	5.9	5.7
	ΔP	−28.9	−27.2	−21.3	−31.8	43.7	−94.0	−33.0	44.3	2.2	4.8	−3.5	−31.6	−7.3	−25.0	−8.7	−11.7
	ΔDSL	26.2	36.1	3.8	20.4	−33.6	134.9	42.7	−19.2	−25.6	−22.9	9.3	31.1	8.5	22.7	63.7	7.3
Zanjan	ΔT_{min}	3.3	3.5	3.7	3.9	4.5	5.0	5.4	5.8	5.7	5.0	4.2	3.6	4.2	3.5	4.5	4.5
	ΔT_{max}	4.1	4.7	4.8	5.4	5.4	6.0	6.3	6.0	6.1	5.1	4.7	4.8	4.9	4.5	5.6	5.3
	ΔP	−9.9	9.1	0.2	−50.9	11.7	−94.7	−66.2	565.6	73.8	40.8	−13.6	−15.6	−4.3	0.2	−22.7	−7.5
	ΔDSL	24.3	42.9	15.0	7.5	12.4	72.6	72.6	−37.8	−14.7	−16.1	3.2	51.1	7.5	27.0	46.8	15.5
Nozheh	ΔT_{min}	3.6	3.9	3.9	4.3	5.0	5.6	5.7	6.1	6.1	5.4	4.5	4.0	4.6	3.8	4.9	4.8
	ΔT_{max}	4.5	5.2	5.2	5.7	5.8	6.4	6.4	6.2	6.4	5.7	5.0	5.2	5.3	4.9	6.0	5.7
	ΔP	−8.4	−18.8	−4.1	−22.2	18.0	−91.9	95.9	1079.	55.2	31.5	13.7	−23.8	0.6	−9.9	−5.5	−2.5
	ΔDSL	11.1	19.6	12.6	20.3	7.0	59.3	7.6	−45.5	−19.7	−7.2	4.7	19.5	4.1	14.3	42.9	9.9
Qazvin	ΔT_{min}	3.1	3.5	3.6	3.8	4.4	4.9	5.3	5.7	5.6	4.9	4.1	3.6	4.2	3.4	4.4	4.4
	ΔT_{max}	4.0	4.6	4.7	5.1	5.6	5.8	6.0	6.1	6.0	5.2	4.6	4.6	4.8	4.4	5.5	5.2
	ΔP	−9.1	−31.0	−4.5	−6.9	−27.8	−74.8	10.5	21.0	141.0	83.5	−11.4	−25.1	−0.1	−14.0	−17.1	−8.7
	ΔDSL	21.5	11.6	−11.2	5.0	21.2	29.7	−9.6	−16.5	−21.8	−8.8	−1.0	−4.5	−5.0	7.9	23.3	2.4
Sanandaj	ΔT_{min}	3.8	3.9	4.0	4.5	5.1	5.7	5.9	6.2	6.5	5.6	4.6	4.1	4.8	3.9	5.1	5.0
	ΔT_{max}	4.7	5.2	5.2	5.8	6.0	6.6	6.5	6.3	6.5	5.6	5.3	5.3	5.4	5.0	6.1	5.8
	ΔP	−20.3	−32.0	−3.8	−30.2	−2.8	−89.8	288.0	148.7	280.5	61.8	−1.6	−35.6	−5.3	−18.3	−21.1	−13.0
	ΔDSL	−1.0	6.4	2.8	8.9	0.1	56.6	−11.7	−35.3	−34.3	−21.8	9.4	3.5	−6.6	2.8	37.4	12.9
Kermanshah	ΔT_{min}	3.8	3.8	4.0	4.5	5.1	5.5	5.7	6.2	6.8	5.9	5.0	4.3	5.1	3.9	5.1	5.1
	ΔT_{max}	5.0	5.0	5.0	5.6	6.0	6.2	6.3	6.4	6.7	6.0	5.6	5.6	5.7	5.0	5.9	5.8
	ΔP	−29.3	−12.0	−21.6	−15.0	−7.4	−27.6	96.6	9.6	5.8	50.2	−6.7	−34.8	−11.2	−21.2	−12.2	−15.6
	ΔDSL	45.4	15.6	9.6	10.1	19.7	24.3	−8.6	−11.9	−17.5	−4.3	15.8	28.4	10.2	22.9	20.5	17.2
Khorramabad	ΔT_{min}	3.8	4.1	4.1	4.9	5.4	5.6	5.8	6.1	6.6	5.9	5.1	4.4	5.1	4.0	5.3	5.1
	ΔT_{max}	5.0	5.2	5.1	5.8	6.0	6.2	6.3	6.1	6.3	5.7	5.5	5.3	5.5	5.0	6.0	5.7
	ΔP	−15.3	−19.8	9.0	0.2	13.3	−35.2	1.7	−66.3	−0.1	1.6	−21.9	−23.2	−19.5	−9.1	3.9	−9.6
	ΔDSL	44.6	28.3	13.7	25.5	26.8	26.9	−11.8	−12.2	−30.7	−15.4	31.6	35.7	9.4	27.8	26.6	18.6

[a] October–November–December.
[b] January–February–March.
[c] April–May–June.

respectively, at Nozheh followed by 0.76 and 1.05 under RCP-4.5 and RCP-8.5, respectively, in Khoy.

The entire growing season precipitation (GSP) change due to shift in planting date within the considered sowing window is unlikely to be considerable (Fig. 3). However, as given in Fig. 3, precipitation change at different phenological stages is significant when the seeding date was changed. In the most stations, the G-TS rainfall was projected to be linearly increased when the planting date was changed from 1 October to BPD. The G-TS rainfall change is likely to be plateaued as the sowing date was shifted later than BPD. Precipitation change at TS-ELG phase exhibits an increasing-decreasing trend within the considered sowing window peaking in BPD (Fig. 3). Averaged across all sites, shifting from CPD to BPD will increase rainfall amount (mm) at TS-ELG phase by 39.2 and 14.9 and within G-TS phase by 12.5 and 27.3 for RCP-4.5 and RCP-8.5, respectively. At most scenarios and locations, rainfall received over ELG-EEG, EEG-BGF and GF stages was predicted to decrease when the seeding date was shifted in weekly interval from the beginning to the end of the considered window. The average precipitation is anticipated to decline (mm) during ELG-EEG by 21.4 and 17.6, EEG-BGF by 11.1 and 13.9 and GF by 12.3 and 7.2 under RCP-4.5 and RCP-8.5, respectively, due to shifting from CPD to BPD. Increase in the G-TS rainfall as a consequence of shift in sowing date to BPD will ensure the adequate crop emergence and establishment. Further, germination kill (a type of crop failure simulated by the model owing to early growing season drought) would be avoided due to the G-TS precipitation increase. An enhancement in the TS-ELG rainfall seems to have positive influences on leaf growth (LAI) and above-ground biomass. It should be noted that LAI is in its maximum value by the end of TS-ELG stage. Increase of LAI as a result of postponing planting date to BPD will shift vapor flux from E to T in the soil-plant-atmosphere system, enhancing T/ET and consequently the produced yield (Ferretti et al., 2003; Rockström, 2003; Rockström and Falkenmark, 2000). This is crucially important in dryland agriculture in which yield improvement through increasing WUE and transpiration share in total water use (ET) is greatly desired (Rockström et al., 2010; Stewart and Steiner, 1990; Yang et al., 2015). Further, leaf growth of wheat (a C3 plant) will be more stimulated by CO_2 fertilization under wetter soil condition during TS-ELG. At the most cases, the greatest precipitation decrease was projected in TS-ELG phase under CPD (Fig. 3). Therefore, the rainfall deficit within the period of TS-ELG can be considered as the most limiting factor for rainfed wheat production in the 2080s. It seems that an increase in the TS-ELG rainfall can remarkably improve rainfed wheat transpiration and yield under CC. In the most sites, the trend of changes in wheat yield and the TS-ELG precipitation was similar when the sowing date was changed within the considered planting window (Fig. 3). Furthermore, harvest loss would

increase when the planting date was shifted later than BPD. This can be explained by a considerable decrease of precipitation at TS-ELG, ELG-EEG, EEG-BGF and GF phases in the most studied stations (Fig. 3).

In the most cases, decline of precipitation during productive period particularly grain filling (a drought-sensitive stage) under BPD is not expected to be significant during the 2080s (Fig. 3). A serious wheat yield loss due to terminal drought seems not, therefore, to be occurred. In addition, a major increase in above-ground biomass through vapor shift may result in a small increase of ET (total water use) in low-yielding regions (such as our study area) due to the trade-off existing between E and T (Asseng et al., 2001). Consequently, increase of biomass during pre-anthesis stages appears not to cause late season drought and harvest loss (Anderson, 1992; Asseng et al., 2001). Moreover, translocation of pre-anthesis carbohydrate to grain can prevent appreciable yield loss (Anderson, 1992; Dodig et al., 2015; Fischer, 1979).

4. Conclusions

The impacts of climate change on rainfed wheat yield, transpiration to total evapotranspiration ratio (T/ET) and maximum leaf area index (LAIm) over a range of sowing dates under RCP-4.5 and RCP-8.5 during 2071–2100 were investigated. In the most studied sites, yield, LAIm and T/ET are expected to decrease under the current planting date (CPD). In the most investigated areas, autumn and winter droughts can account for reduction of yield, LAIm and T/ET. Precipitation at two early stages i.e. germination to terminal spikelet initiation (G-TS) and terminal spikelet to end of leaf growth and beginning of ear phases (TS-ELG) will increase when sowing was delayed from the current to the best date. Enhanced G-TS rainfall would benefit crop establishment and decrease the probability of crop failure during early growing season. Precipitation increment during TS-ELG would also lead to increased LAI and T/ET. Moreover, a great decline of rainfall at grain filling stage (GF) and entire growing season is not anticipated due to delay-

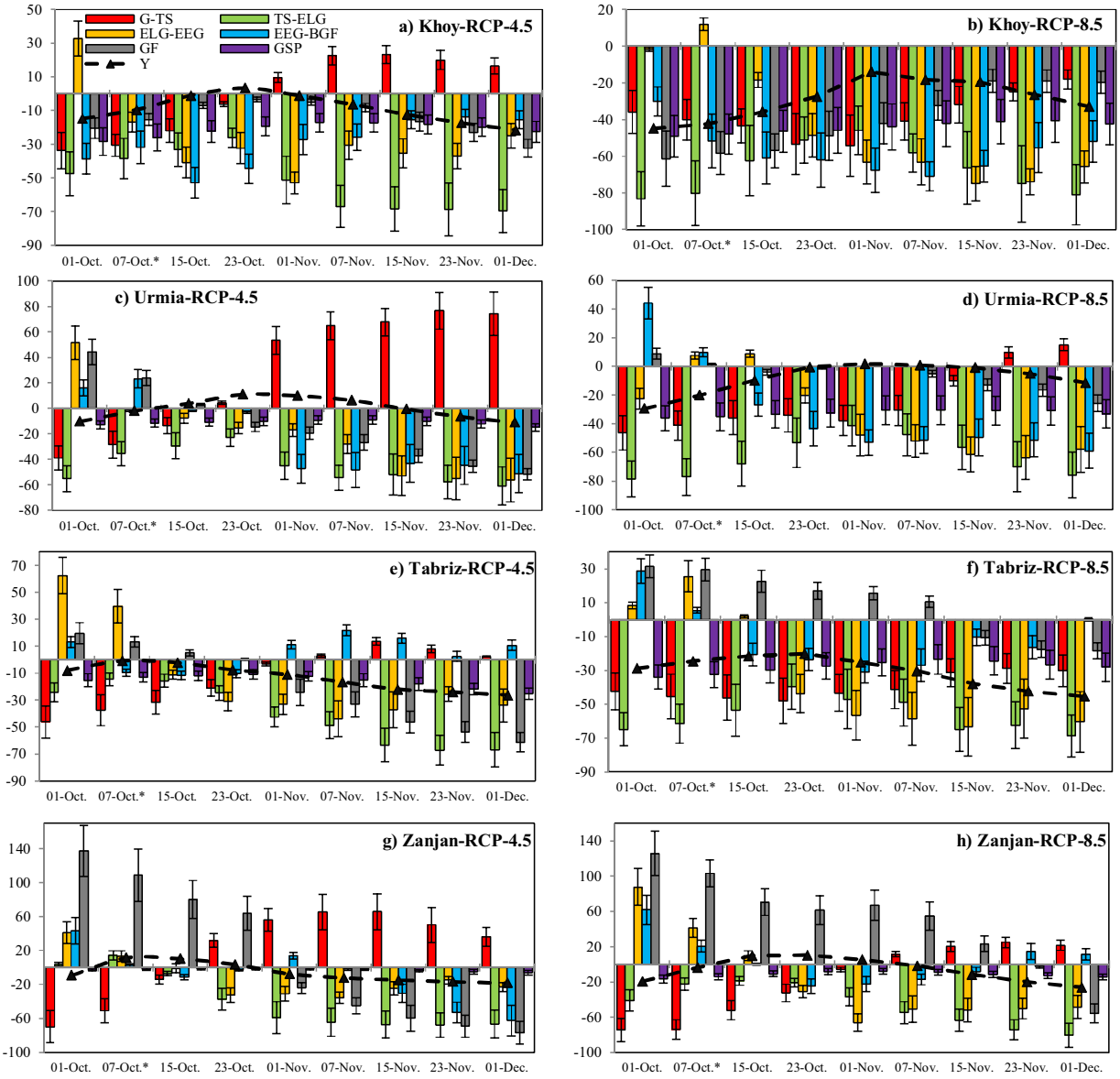

Fig. 3. The changes (%) in wheat yield (Y) and precipitation at germination to terminal spikelet initiation (G-TS), terminal spikelet to end of leaf growth and beginning of ear growth (TS-ELG), end of leaf growth and beginning of ear growth to end of pre-anthesis ear growth (ELG-EEG), end of pre-anthesis ear growth to beginning of grain filling (EEG-BGF) and grain filling (GF) stages over a wide range of planting dates under RCP-4.5 and 8.5 in the 2080s relative to the baseline. (The asterisk denotes the current sowing date) (The asterisk denotes the current sowing date. Error bars show the standard deviation of the projections).

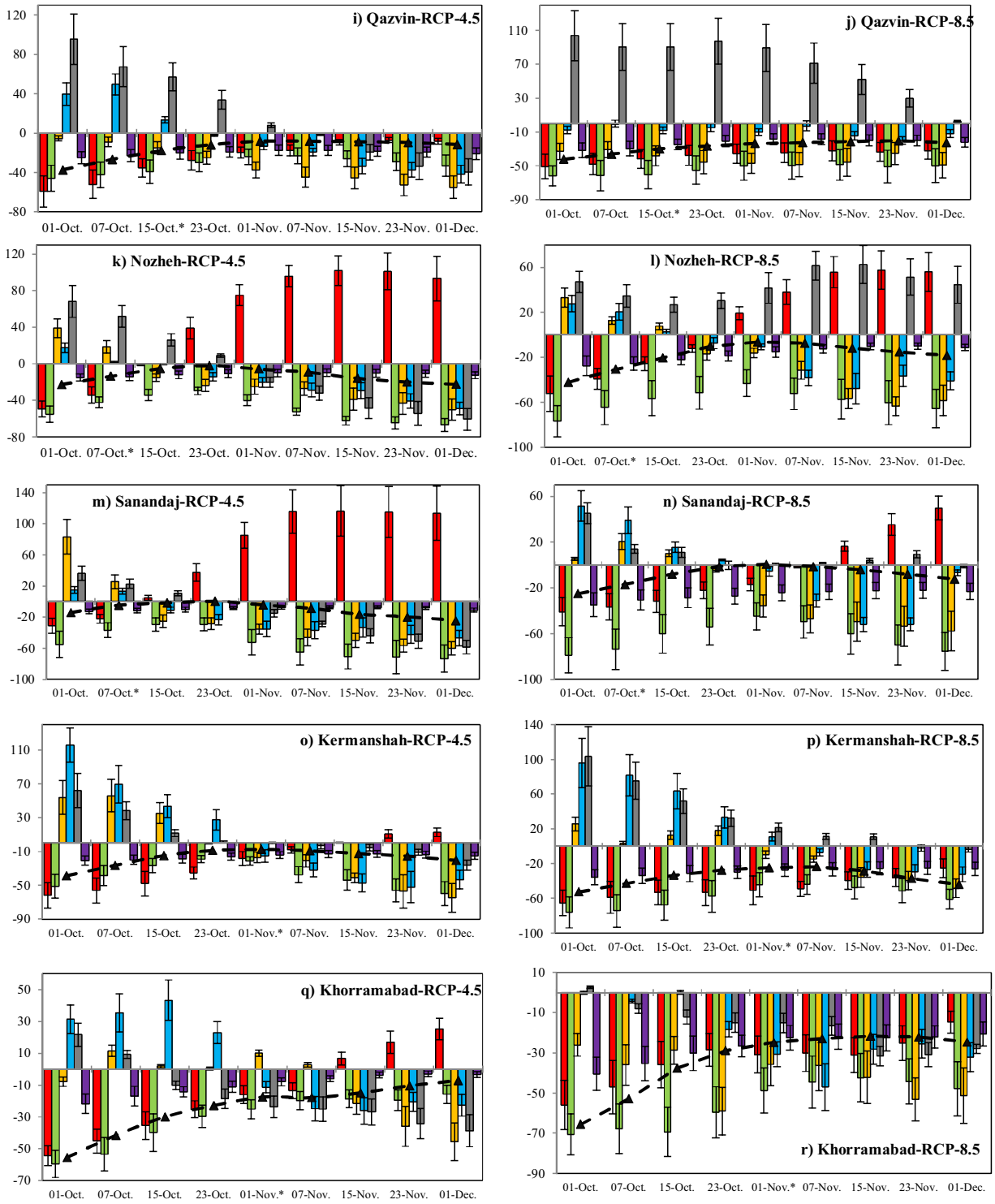

Fig. 3. The(it Continued)

ing planting date. Delay in sowing date would, therefore, match crop development with changed rainfall distribution in the 2080s. As a result, postponing planting date as an adaptive strategy can enhance productive water loss (transpiration) and partially compensate rainfed winter wheat yield loss in the last 30 years of the 21st century. The uncertainties of the results need to be taken into account by decision makers.

Acknowledgment

The authors appreciate Iran Soil and Water Research Institute (SWRI) and Iran Meteorological Organization (IRIMO) for their collaboration in making required literature and data available. They also thank Vali Feiziasl and Abdollali Ghafari from the Iranian Dryland Agricultural Research Institute (DARI) for providing some data and their worthwhile comments.

References

Anderson, W., 1992. Increasing grain yield and water use of wheat in a rainfed Mediterranean type environment. Crop Pasture Sci. 43, 1–17.

Anwar, M.R., O'Leary, G., McNeil, D., Hossain, H., Nelson, R., 2007. Climate change impact on rainfed wheat in south-eastern Australia. Field Crops Res. 104, 139–147.

Asseng, S., Turner, N., Keating, B.A., 2001. Analysis of water- and nitrogen-use efficiency of wheat in a Mediterranean climate. Plant Soil 233, 127–143.

Collins, M., Knutti, R., Arblaster, J., Dufresne, J.-L., Fichefet, T., Friedlingstein, P., Gao, X., Gutowski, W.J., Johns, T., Krinner, G., Shongwe, M., Tebaldi, C., Weaver, A., Wehner, M., 2013. Long-term climate change: projections, commitments and irreversibility. In: Stocker, T.F., Qin, D., Plattner, G.-K., Tignor, M.B.T., Allen, S.K., Boschung, J., Nauels, A., Xia, Y., Bex, V., Midgley, P.M. (Eds.), Climate Change 2013: The Physical Science Basis. Contribution of Working Group I to the Fifth Assessment Report of the Intergovernmental Panel on Climate Change. Cambridge University Press, Cambridge, United Kingdom/New York, NY, USA, pp. 1029–1136.

Dai, A., 2011. Drought under global warming: a review. Wiley Interdiscip. Rev.: Clim. Change 2, 45–65.

Dai, A., 2013. Increasing drought under global warming in observations and models. Nat. Clim. Change 3, 52–58.

DARI, 2014. Technical Instruction of Rainfed Wheat Cultivation in Different Climatic Zones of Iran. Ministry of Agriculture, Research and Education Organization, Dryland Agricultural Research Institute (DARI), Iran, pp. 31 (in Persian).

Delécolle, R., Ruget, F., Ripoche, D., Gosse, G., 1995. Possible effects of climate change on wheat and maize crops in France. In: Rosenzweig, C. (Ed.), Climate Change and Agriculture: Analysis of Potential International Impacts. American Society of Agronomy, Madison, WI.

Dettori, M., Cesaraccio, C., Motroni, A., Spano, D., Duce, P., 2011. Using CERES-Wheat to simulate durum wheat production and phenology in Southern Sardinia, Italy. Field Crops Res. 120, 179–188.

Dodig, D., Savić, J., Kandić, V., Zorić, M., Vucelić radović, B., Popović, A., Quarrie, S., 2015. Responses of wheat plants under post-anthesis stress induced by defoliation: I. Contribution of agro-physiological traits to grain yield. Exp. Agric. FirstView, 1–21.

Dufresne, J.-L., Foujols, M.-A., Denvil, S., Caubel, A., Marti, O., Aumont, O., Balkanski, Y., Bekki, S., Bellenger, H., Benshila, R., 2013. Climate change projections using the IPSL-CM5 Earth System Model: from CMIP3 to CMIP5. Clim. Dyn. 40, 2123–2165.

Dunne, J.P., John, J.G., Adcroft, A.J., Griffies, S.M., Hallberg, R.W., Shevliakova, E., Stouffer, R.J., Cooke, W., Dunne, K.A., Harrison, M.J., 2012. GFDL's ESM2 global coupled climate-carbon Earth System Models. Part I: Physical formulation and baseline simulation characteristics. J. Clim. 25, 6646–6665.

Evans, J.P., 2009. 21st century climate change in the Middle East. Clim. Change 92, 417–432.

Eyshi Rezaie, E., Bannayan, M., 2012. Rainfed wheat yields under climate change in northeastern Iran. Meteorol. Appl. 19, 346–354.

Falkenmark, M., 2013. Adapting to climate change: towards societal water security in dry-climate countries. Int. J. Water Resour. Dev. 29, 123–136.

Faures, J.-M., Svendsen, M., Turral, H., Berkhoff, J., Bhattarai, M., Caliz, A., Darghouth, S., Doukkali, M., El-Kady, M., Facon, T., 2007. Reinventing irrigation. In: Molden, D. (Ed.), Water for Food Water for Life: A Comprehensive Assessment of Water Management in Agriculture. Earthscan/International Water Management Institute, London/Colombo, pp. 585–625.

Feiziasl, V., Toshieh, V., Esmaeilie, M., 2007. Study on the Effects of Different Sources and Rates of Soil Nitrogen on Quality and Quantities of Rain Fed Wheat. Ministry of Agriculture, Research and education organization, Dryland Agricultural Research Institute (DARI), Iran, pp. 148 (in Persian).

Ferretti, D., Pendall, E., Morgan, J., Nelson, J., Lecain, D., Mosier, A., 2003. Partitioning evapotranspiration fluxes from a Colorado grassland using stable isotopes: seasonal variations and ecosystem implications of elevated atmospheric CO_2. Plant Soil 254, 291–303.

Fischer, G., Shah, M., Van Velthuizen, H., 2002. Climate Change and Agricultural Vulnerability. Special Report for the UN World Summit on Sustainable Development, 26 August–4 September. International Institute for Applied Systems Analysis, Johannesburg, Laxenburg, Austria152.

Fischer, R., 1979. Growth and water limitation to dryland wheat yield in Australia: a physiological framework. J. Aust. Inst. Agric. Sci. 45, 83–94.

Flato, G., Marotzke, J., Abiodun, B., Braconnot, P., Chou, S.C., Collins, W.J., Cox, P., Driouech, F., Emori, S., Eyring, V., 2013. Evaluation of climate models. In: Stocker, T.F., Qin, D., Plattner, G.-K., Tignor, M.B.T., Allen, S.K., Boschung, J., Nauels, A., Xia, Y., Bex, V., Midgley, P.M. (Eds.), Climate Change 2013: The Physical Science Basis. Contribution of Working Group I to the Fifth Assessment Report of the Intergovernmental Panel on Climate Change. Cambridge University Press, Cambridge, United Kingdom/New York, NY, USA, pp. 741–866.

Fouial, A., Khadra, R., Daccache, A., Lamaddalena, N., 2016. Modelling the impact of climate change on pressurised irrigation distribution systems: use of a new tool for adaptation strategy implementation. Biosyst. Eng. 150, 182–190.

Ghahramani, A., Kokic, P.N., Moore, A.D., Zheng, B., Chapman, S.C., Howden, M.S., Crimp, S.J., 2015. The value of adapting to climate change in Australian wheat farm systems: farm to cross-regional scale. Agric. Ecosyst. Environ. 211, 112–125.

Homaee, M., Dirksen, C., Feddes, R., 2002a. Simulation of root water uptake: I. Non-uniform transient salinity using different macroscopic reduction functions. Agric. Water Manag. 57, 89–109.

Homaee, M., Feddes, R., Dirksen, C., 2002b. A macroscopic water extraction model for nonuniform transient salinity and water stress. Soil Sci. Soc. Am. J. 66, 1764–1772.

Homaee, M., Feddes, R., Dirksen, C., 2002c. Simulation of root water uptake: II. Non-uniform transient water stress using different reduction functions. Agric. Water Manag. 57, 111–126.

Homaee, M., Feddes, R., Dirksen, C., 2002d. Simulation of root water uptake: III. Non-uniform transient combined salinity and water stress. Agric. Water Manag. 57, 127–144.

Homaee, M., Schmidhalter, U., 2008. Water integration by plants root under non-uniform soil salinity. Irrig. Sci. 27, 83–95.

Hoogenboom, G., Jones, J.W., Wilkens, P.W., Porter, C.H., Boote, K.J., Hunt, L.A., Singh, U., Lizaso, J.I., White, J.W., Uryasev, O., Ogoshi, R., Koo, J., Shelia, V., Tsuji, G.Y., 2014. Decision Support System for Agrotechnology Transfer (DSSAT) Version 4.6. DSSAT Foundation Prosser, Washington, www.DSSAT.net.

IPCC, 2013. In: Stocker, T.F., Qin, D., Plattner, G.-K., Tignor, M.B.T., Allen, S.K., Boschung, J., Nauels, A., Xia, Y., Bex, V., Midgley, P.M. (Eds.), Climate Change 2013: The Physical Science Basis. Contribution of Working Group I to the Fifth Assessment Report of the Intergovernmental Panel on Climate Change. Cambridge University Press, Cambridge, United Kingdom/New York, NY, USA, p. 1535.

Jones, J.W., Hoogenboom, G., Porter, C.H., Boote, K.J., Batchelor, W.D., Hunt, L., Wilkens, P.W., Singh, U., Gijsman, A.J., Ritchie, J.T., 2003. The DSSAT cropping system model. Eur. J. Agron. 18, 235–265.

Jones, P.G., Thornton, P.K., 2013. Generating downscaled weather data from a suite of climate models for agricultural modelling applications. Agric. Syst. 114, 1–5.

Li, Y., Ye, W., Wang, M., Yan, X., 2009. Climate change and drought: a risk assessment of crop-yield impacts. Clim. Res. 39, 31.

Liu, Y., Theller, L.O., Pijanowski, B.C., Engel, B.A., 2016. Optimal selection and placement of green infrastructure to reduce impacts of land use change and climate change on hydrology and water quality: an application to the Trail Creek Watershed, Indiana. Sci. Total Environ. 553, 149–163.

Mathukumalli, S.R., Dammu, M., Sengottaiyan, V., Ongolu, S., Biradar, A.K., Kondru, V.R., Karlapudi, S., Bellapukonda, M.K.R., Chitiprolu, R.R.A., Cherukumalli, S.R., 2016. Prediction of *Helicoverpa armigera* Hubner on pigeonpea during future climate change periods using MarkSim multimodel data. Agric. Forest Meteorol. 228–229, 130–138.

Ministry of Agriculture, 2011. Statistics of Agricultural Products, Crop Production in 2009–2010. Office of Statistics and Information Technology, Ministry of Agriculture, Tehran, Iran.

Molle, F., Wester, P., Hirsch, P., Jensen, J.R., Murray-Rust, H., Paranjpye, V., Pollard, S., Van der Zaag, P., 2007. River basin development and management. In: Molden, D. (Ed.), Water for Food Water for Life: A Comprehensive Assessment of Water Management in Agriculture. International Water Management Institute/Earthscan, London/Colombo, pp. 584–624.

Nouri, M., Homaee, M., Bannayan, M., Hoogenboom, G., 2016. Towards modeling soil texture-specific sensitivity of wheat yield and water balance to climatic changes. Agric. Water Manag. 177, 248–263.

Nouri, M., Homaee, M., Bybordi, M., 2014. Quantitative assessment of LNAPL retention in soil porous media. Soil Sedim. Contam. 23, 801–819.

Rawls, W., Brakensiek, D., Saxton, K., 1982. Estimation of soil water properties. Trans. ASAE 25, 1316–1320.

Riahi, K., Rao, S., Krey, V., Cho, C., Chirkov, V., Fischer, G., Kindermann, G., Nakicenovic, N., Rafaj, P., 2011. RCP 8.5—a scenario of comparatively high greenhouse gas emissions. Clim. Change 109, 33–57.

Richardson, C.W., 1981. Stochastic simulation of daily precipitation, temperature, and solar radiation. Water Resour. Res. 17, 182–190.

Ritchie, J.T., 1972. Model for predicting evaporation from a row crop with incomplete cover. Water Resour. Res. 8, 1204–1213.

Ritchie, J.T., 1991. Wheat phasic development. In: Hanks, J., Ritchie, J.T. (Eds.), Modeling Plant and Soil Systems. American Society of Agronomy, Crop Science Society of America, Soil Science Society of America, Madison, WI.

Ritchie, J.T., 1998. Soil water balance and plant water stress. In: Tsuji, G., Hoogenboom, G., Thornton, P. (Eds.), Understanding Options for Agricultural Production. Springer, Netherlands, pp. 41–54.

Rockström, J., 2003. Water for food and nature in drought-prone tropics: vapour shift in rain-fed agriculture. Philos. Trans. R. Soc. B: Biol. Sci. 358, 1997–2009.

Rockström, J., Falkenmark, M., 2000. Semiarid crop production from a hydrological perspective: gap between potential and actual yields. Crit. Rev. Plant Sci. 19, 319–346.

Rockström, J., Falkenmark, M., Karlberg, L., Hoff, H., Rost, S., Gerten, D., 2009. Future water availability for global food production: the potential of green water for increasing resilience to global change. Water Resour. Res. 45.

Rockström, J., Hatibu, N., Oweis, T., Wani, S., Barron, J., Bruggeman, A., Qiang, Z., Farahani, J., Karlberg, L., 2007. Managing water in rainfed agriculture. In: Molden, D.E. (Ed.), Water for Food Water for Life: A Comprehensive Assessment of Water Management in Agriculture. Earthscan/International Water Management Institute, London/Colombo, pp. 311–352.

Rockström, J., Karlberg, L., Wani, S.P., Barron, J., Hatibu, N., Oweis, T., Bruggeman, A., Farahani, J., Qiang, Z., 2010. Managing water in rainfed agriculture—the need for a paradigm shift. Agric. Water Manag. 97, 543–550.

Rosenzweig, C., 1990. Crop response to climate change in the southern Great Plains: a simulation study. Prof. Geogr. 42, 20–37.

Saadat, S., Homaee, M., 2015. Modeling sorghum response to irrigation water salinity at early growth stage. Agric. Water Manag. 152, 119–124.
Sau, F., Boote, K.J., Bostick, W.M., Jones, J.W., Mínguez, M.I., 2004. Testing and improving evapotranspiration and soil water balance of the DSSAT crop models. Agron. J. 96, 1243–1257.
Saxton, K., Rawls, W.J., Romberger, J., Papendick, R., 1986. Estimating generalized soil-water characteristics from texture. Soil Sci. Soc. Am. J. 50, 1031–1036.
Shirsath, P.B., Aggarwal, P.K., Thornton, P.K., Dunnett, A., 2017. Prioritizing climate-smart agricultural land use options at a regional scale. Agric. Syst. 151, 174–183.
Song, Z., Qiao, F., Song, Y., 2012. Response of the equatorial basin-wide SST to non-breaking surface wave-induced mixing in a climate model: an amendment to tropical bias. J. Geophys. Res.: Oceans 117, C00J26.
Southworth, J., Pfeifer, R., Habeck, M., Randolph, J., Doering, O., Rao, D.G., 2002. Sensitivity of winter wheat yields in the Midwestern United States to future changes in climate, climate variability, and CO_2 fertilization. Clim. Res. 22, 73–86.
Stewart, B.A., Steiner, J.L., 1990. Water-use efficiency. In: Singh, R.P., Parr, J.F., Stewart, B.A. (Eds.), Advances in Soil Science Dryland Agriculture: Strategies for Sustainability, vol. 13. Springer, New York, pp. 151–173.
Thomson, A.M., Calvin, K.V., Smith, S.J., Kyle, G.P., Volke, A., Patel, P., Delgado-Arias, S., Bond-Lamberty, B., Wise, M.A., Clarke, L.E., 2011. RCP4.5: a pathway for stabilization of radiative forcing by 2100. Clim. Change 109, 77–94.
Torriani, D., Calanca, P.-L., Schmid, S., Beniston, M., Fuhrer, J., 2007. Potential effects of changes in mean climate and climate variability on the yield of winter and spring crops in Switzerland. Clim. Res. 34, 59–69.
Tubiello, F., Rosenzweig, C., Goldberg, R., Jagtap, S., Jones, J., 2002. Effects of climate change on US crop production: simulation results using two different GCM scenarios. Part I: Wheat, potato, maize, and citrus. Clim. Res. 20, 259–270.
Turral, H., Burke, J.J., Faurès, J.-M., 2011. Climate Change, Water and Food Security. FAO Water Reports 36. FAO, Rome.
UNEP, 1997. World Atlas of Desertification, second ed. Arnold, United Nations Environment Programme, London, UK, pp. 182.
Watanabe, S., Hajima, T., Sudo, K., Nagashima, T., Takemura, T., Okajima, H., Nozawa, T., Kawase, H., Abe, M., Yokohata, T., 2011. MIROC-ESM 2010: model description and basic results of CMIP5-20c3m experiments. Geosci. Model Dev. 4, 845–872, http://dx.doi.org/10.5194/gmd-4-845-2011.
Weiss, A., Hays, C.J., Won, J., 2003. Assessing winter wheat responses to climate change scenarios: a simulation study in the US Great Plains. Clim. Change 58, 119–147.
Willmott, C.J., 1982. Some comments on the evaluation of model performance. Bull. Am. Meteorol. Soc. 63, 1309–1313.
Willmott, C.J., Robeson, S.M., Matsuura, K., 2012. A refined index of model performance. Int. J. Climatol. 32, 2088–2094.
Wu, T., 2012. A mass-flux cumulus parameterization scheme for large-scale models: description and test with observations. Clim. Dyn. 38, 725–744.
Yang, Y., Li Liu, D., Anwar, M.R., O'Leary, G., Macadam, I., Yang, Y., 2015. Water use efficiency and crop water balance of rainfed wheat in a semi-arid environment: sensitivity of future changes to projected climate changes and soil type. Theor. Appl. Climatol., 1–15.
Zarei, G., Homaee, M., Liaghat, A.M., Hoorfar, A.H., 2010. A model for soil surface evaporation based on Campbell's retention curve. J. Hydrol. 380, 356–361.